AIMS Mathematics, 11(1): 399–419.
DOI: 10.3934/math.2026017
Received: 24 September 2025
Revised: 16 December 2025
Accepted: 18 December 2025
Published: 06 January 2026

https://www.aimspress.com/journal/Math

Research article

Spectrum of non-trivial zeros, distribution and magnitude of prime numbers

Ilija Tanackov[1,*], Ivan Pavkov[2] , Dejan Ćebić[3] and Željko Stević[4,5,*]

[1] Faculty of Technical Sciences, University of Novi Sad, Trg D. Obradovića 6, Novi Sad, Serbia
[2] Faculty of Agriculture, University of Belgrade, Nemanjina 6, Zemun, Serbia
[3] Faculty of Mining and Geology, University of Belgrade, Đušina 7, Belgrade, Serbia
[4] Department of Industrial Management Engineering, Korea University, Seoul 02841, Republic of Korea
[5] Faculty of Transport and Traffic Engineering, University of East Sarajevo, Doboj 74000, Bosnia and Herzegovina

* **Correspondence:** Email: ilijat@uns.ac.rs, +381607696000; zeljkostevic88@yahoo.com, +38765042093.

Abstract: Spectrum $RCS(n)=\sum\cos(t_j \ln n)$, $j\in[1, \infty)$, based on imaginary values of non-trivial zeros of the zeta function $\zeta(s)=\zeta(½\pm it_j)=0$, $\mathrm{Im}(s)=\pm t_j$, results in "high peaks" (i.e., resonant values of cosine amplitudes at the prime powers $n=p^k$, $k\in\mathbb{N}$ in the negative part of the spectrum). The spectrum of the r^{th} root $RCS(n^{1/r})=\sum\cos(t_j \ln n^{1/r})$, $r\in\mathbb{N}$ exclusively reaches its resonance values in the values of the degree $n=p^r$. Owing to that fact, prime numbers p^1 can be separated from prime powers $p^{1/r}$, $r\geq 2$. The spectrum of the d^{th} degree $RCS(n^d)=\sum\cos(t_j \ln n^d)$, $d\in\mathbb{N}$ exclusively reaches its resonant values exclusively in the values of the root $p^{1/d}$, $d\geq 2$. The spectrum of the d^{th} degree "compresses" the number axis. For an arbitrary real interval (a, b), all the resonances p^d of all prime numbers from the interval (a^d, b^d) are contained in the interval (a, b). The imaginary sine spectrum-*ISS* and the composite spectrum of the *RCS* and *ISS* is developed.

Keywords: Zeta functions; resonances; Riemann hypothesis
Mathematics Subject Classification: 11N05

1. Introduction

According to historical data, Riemann calculated the first six non-trivial zeros [1]. The importance of non-trivial zeros was highlighted in 1900 in Paris, at the promotion of Hilbert's 24 unsolved problems. In 1903, Gram calculated more than 10 non-trivial zeros (15 in total) [2]. In 1925, the limit of 100 (exactly 138) calculated non-trivial zeros was exceeded by J. I. Hutchinson [3]. In 1935, the limit of 1000 was exceeded by Titchmarsh [4]. In 1956, the limit of 10,000 was exceeded by Lehmer [5]. In 1966, the limit of 100000 was reached by Lehman [6]. In 1968, the limit of millions was reached by Rosser, Yohe, and Schoenfeld [7]. In 1977, the limit of 10 million was crossed by Brent [8]. In 1982, the limit of 100 million was crossed by Brent, van de Lune, Riele, and Winter [9]. In 1986, the limit of billion crossed by van de Lune, Riele, and Winter [10]. In 2003, the limit of 100 billion was crossed by Wedeniwski [11]. In 2021, Platt and Trudgian [12] reach a maximum of $3 \cdot 10^{12}$ calculated non-trivial zeros. These calculations were mainly performed for the purpose of expressing the Riemann hypothesis [13]. The Riemann prime counting function indirectly respects non-trivial zeros. It is based on the Möbius function (i.e., by the logarithm of the zeta function). However, the Riemann prime counting function does not directly contain the concept of the distribution of prime numbers.

Although the numerical relationship between prime numbers and non-trivial zeros was highlighted in [14], a graphical presentation of the distribution of p^k numbers was presented through the basic spectrum in [15]. In general, the significant lack of the spectrum is the fact that it highlights the values in p^k, $k \geq 1$ and that there is no concept that would differentiate the prime numbers p^1 from the power of the prime powers p^k, $k \geq 2$.

The density of non-trivial zeros was explored in [16]. The degrees of prime numbers [17] and the number of primes between consecutive prime powers [18] will play an important role for our exploration. The importance of von Mangoldt [19] and the second Chebyshev function [20] will be increased after the presentation of the spectrum of roots and powers. The results related to square roots from [21] inspired the research of the existence of powers and/or roots in the spectra. Furthermore, it led us to the graphical presentation and the establishment of the prime number distribution function.

From the results of [15,21], the possibility of developing a wider class of spectra is observed. The main novelty in this paper is the distribution and magnitudes of prime numbers based on the spectrum of roots and powers.

2. The genesis of the real cosine spectrum-*RCS*

The basic real cosine spectrum equation for the value of n and non-trivial zeros t_1=14.134725..., t_2=21.022039..., t_3=25.010857..., etc. from [15] is given by (1):

$$RCS(n) = \sum_{j=1}^{\infty} \cos(t_j \ln n). \tag{1}$$

Equation (1) can be transformed in the following way (2):

$$RCS(n)=\frac{1}{2}\sum_{j=1}^{\infty}2\cos(t_j\ln n)=\frac{1}{2}\sum_{j=1}^{\infty}\frac{2\cos(t_j\ln n)+i(\overbrace{\sin(t_j\ln n)-\sin(t_j\ln n)}^{=0})}{n^0}$$
$$=\frac{1}{2}\sum_{j=1}^{\infty}\left(\frac{\cos(t_j\ln n)+i\sin(t_j\ln n)}{n^0}+\frac{\cos(t_j\ln n)-i\sin(t_j\ln n)}{n^0}\right). \tag{2}$$

Furthermore,

$$\sum_{n=1}^{\infty}RCS(n)=\frac{1}{2}\sum_{n=1}^{\infty}\sum_{j=1}^{\infty}\left(\frac{\cos(t_j\ln n)+i\sin(t_j\ln n)}{n^0}+\frac{\cos(t_j\ln n)-i\sin(t_j\ln n)}{n^0}\right)$$
$$=\sum_{j=1}^{\infty}\frac{\zeta(0+it_j)+\zeta(0-it_j)}{2}. \tag{3}$$

The most important spectrum identities are provided in Table 1.

Table 1. Basic identity of the *RCS* and the zeta function.

	t_1=14.13472...	t_2=21.02203...	t_3=25.01085...	...	$\sum$
n=1	$\cos(t_1\ln 1)$	$\cos(t_2\ln 1)$	$\cos(t_3\ln 1)$	...	$RCS(1)=\sum_{i=1}^{\infty}\cos(t_i\ln 1)$
n=2	$\cos(t_1\ln 2)$	$\cos(t_2\ln 2)$	$\cos(t_3\ln 2)$	...	$RCS(2)=\sum_{i=1}^{\infty}\cos(t_i\ln 2)$
n=3	$\cos(t_1\ln 3)$	$\cos(t_2\ln 3)$	$\cos(t_3\ln 3)$	...	$RCS(3)=\sum_{i=1}^{\infty}\cos(t_i\ln 3)$
n=4	$\cos(t_1\ln 4)$	$\cos(t_2\ln 4)$	$\cos(t_3\ln 4)$	...	$RCS(4)=\sum_{i=1}^{\infty}\cos(t_i\ln 4)$
...	...	...	...	...	...
$\sum$	$\frac{\zeta(+it_1)+\zeta(-it_1)}{2}$	$\frac{\zeta(+it_2)+\zeta(-it_2)}{2}$	$\frac{\zeta(it_3)+\zeta(-it_3)}{2}$	...	$\sum_{n=1}^{\infty}\sum_{i=1}^{\infty}\cos(t_i\ln n)$

As $Re(s)=0$, there is the possibility of the existence of spectrums with arguments that are proportional to the non-trivial zeros (4). For the spectrum of root $r\in\mathbb{N}$ and the spectrum of degree $d\in\mathbb{N}$ (4), the following holds:

$$\frac{1}{2}\sum_{j=1}^{\infty}\sum_{n=1}^{\infty}\left(\frac{1}{n^{+\frac{it_j}{r}}}+\frac{1}{n^{+\frac{it_j}{r}}}\right)=\sum_{j=1}^{\infty}\frac{\zeta\left(\frac{+it_j}{r}\right)+\zeta\left(\frac{-it_j}{r}\right)}{2}=\sum_{n=1}^{\infty}\sum_{j=1}^{\infty}\cos(\frac{t_j}{r}\ln n)=\sum_{n=1}^{\infty}\sum_{j=1}^{\infty}\cos(t_j\ln\sqrt[r]{n}),$$
$$\frac{1}{2}\sum_{j=1}^{\infty}\sum_{n=1}^{\infty}\left(\frac{1}{n^{+it_jd}}+\frac{1}{n^{-it_jd}}\right)=\sum_{i=1}^{\infty}\frac{\zeta(+it_jd)+\zeta(0-it_jd)}{2}=\sum_{n=1}^{\infty}\sum_{j=1}^{\infty}\cos(dt_j\ln n)=\sum_{n=1}^{\infty}\sum_{j=1}^{\infty}\cos(t_j\ln n^d). \quad (4)$$

Key values for spectrum calculations are the imaginary parts of non-trivial zeros Im(s)=±t_j; however, for the values of the real part on Re(s)=0 that do not lie on the critical axis (i.e., $\zeta(0\pm it_j)$), values of the zeta function for Re(s)≠½ are also significant for the distribution of prime numbers.

3. Resultant spectrum of prime numbers

3.1. Basic spectrum r=d=1

Based on the first 100000 non-trivial zeros from [2] (t_1=14.134725, t_2=21.022039, t_3=25.010857,..., t_{100}=236.524229,..., t_{1000}=1419.422480,..., t_{10000}=9877.782654,..., t_{50000}=40,433.687385,..., t_{100000}=74,920.827498) in form (5), the spectrum was formed in the interval [1, 256]. The calculation interval (increment) is Δ=0.1.

There are 54 prime numbers in the selected interval: 2, 3, 5, 7, 11, 13, 17, 19, 23, 29, 31, 37, 41, 43, 47, 53, 59, 61, 67, 71, 73, 79, 83, 89, 97, 101, 103, 107, 109, 113, 127, 131, 137, 139, 149, 151, 157, 163, 167, 173, 179, 181, 191, 193, 197, 199, 211, 223, 227, 229, 233, 239, 241, and 251.

In addition to the prime numbers, there are 16 composite numbers within this interval: 2^2=4, 2^3=8, 2^4=16, 2^5=32, 2^6=64, 2^7=128, 2^8=256, 3^2=9, 3^3=24, 3^4=81, 3^5=243, 5^2=25, 5^3=125, 7^2=49, 11^2=121, and 13^2=169.

All 60 mentioned numbers have pronounced resonances in the negative part of the *RCS*. Figure 1 shows a graphical representation of the *RCS* with enlarged details in the intervals [1, 30] and [120, 140]. It is well known that the absolute values of resonances of prime numbers p^1 are greater than the absolute values of resonances of composite numbers p^k, k≥2. All resonances are exclusively located over the integers that are in the form p^k, k≥1 (5):

$$RCS(n)=\sum_{j=1}^{10^5}\cos(t_j\ln n). \quad (5)$$

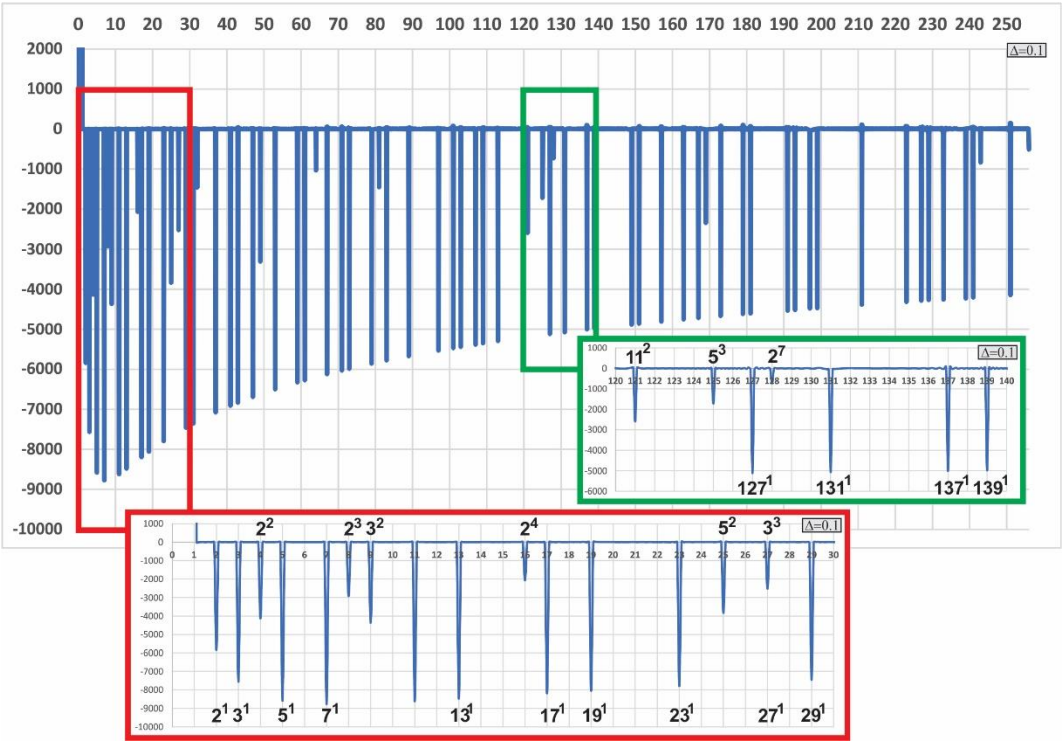

Figure 1. Basic *RCS*.

3.2. RCS of roots and distribution of prime numbers

The *RCS* of the square root of the argument n (6) is shown in Figure 2. The resonances for numbers 4, 9, 16, 25, 49, 64, 81, 121, 169, and 256 are established.

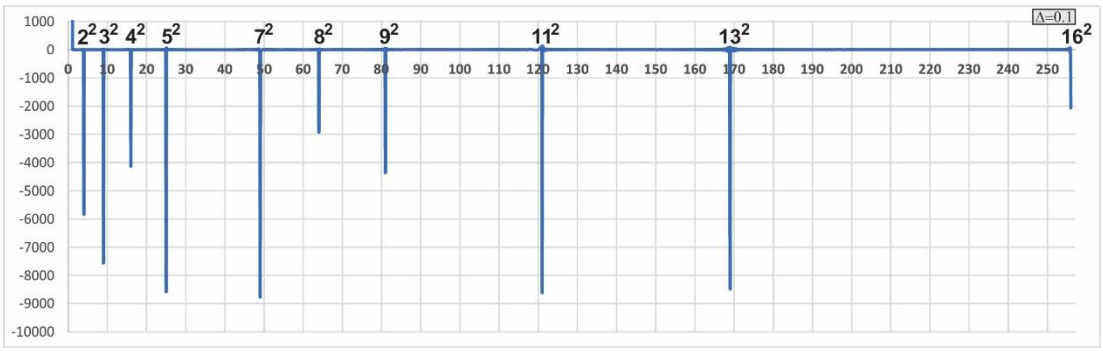

Figure 2. *RCS* of the square root.

$$RCS(\sqrt{n}) = \sum_{j=1}^{10^5} \cos(t_j \ln\sqrt{n}) = \sum_{j=1}^{10^5} \cos\frac{t_j \ln n}{2}. \tag{6}$$

The *RCS* of the third root of the argument n (7) is shown in Figure 3. Resonances of the third degree of prime powers are established (i.e., 2^3, 3^3, 4^3 and 5^3):

$$RCS(\sqrt[3]{n}) = \sum_{j=1}^{10^5} \cos(t_j \ln \sqrt[3]{n}) = \sum_{j=1}^{10^5} \cos \frac{t_j \ln n}{3}. \tag{7}$$

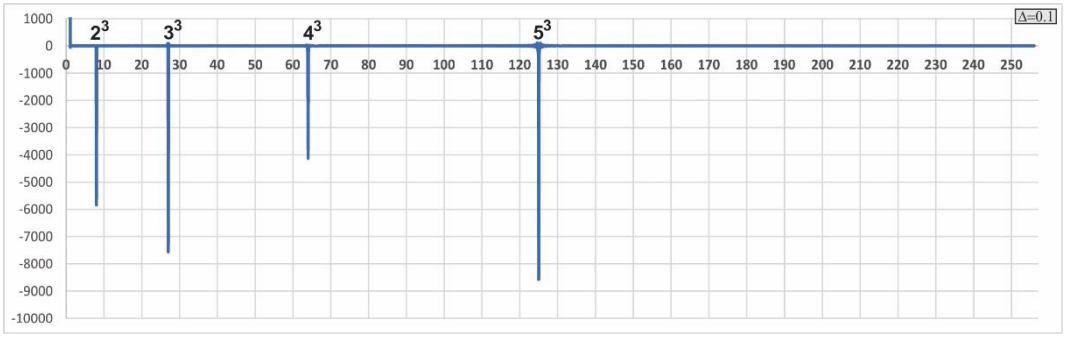

Figure 3. *RCS* of the third root.

The *RCS* of the fourth root of the argument n (8) is shown in Figure 4. Resonants of the fourth power of prime powers are established (i.e., 2^4, 3^4 and 4^4):

$$RCS(\sqrt[4]{n}) = \sum_{j=1}^{10^5} \cos(t_j \ln \sqrt[4]{n}) = \sum_{j=1}^{10^5} \cos \frac{t_j \ln n}{4}. \tag{8}$$

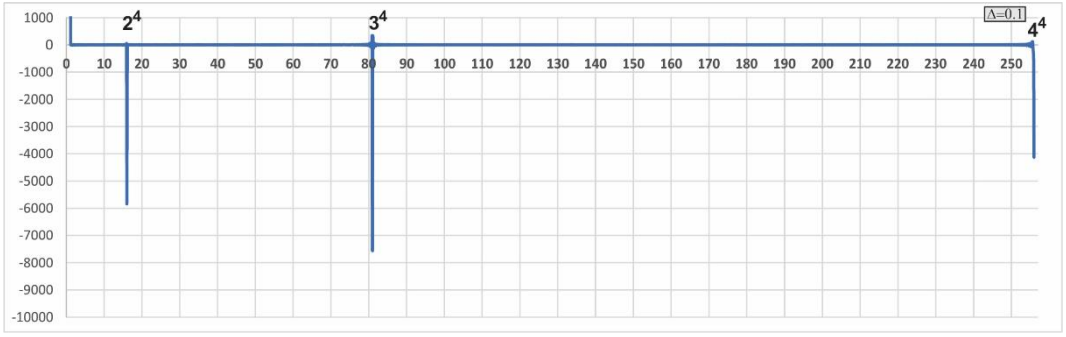

Figure 4. *RCS* of the fourth root.

The *RCS* of the fifth root of the argument n (9) is shown in Figure 5. Enlarged intervals [30,40] and [240,250] highlight resonances in 2^5 and 3^5 in that order:

$$RCS(\sqrt[5]{n}) = \sum_{j=1}^{10^5} \cos(t_j \ln \sqrt[5]{n}) = \sum_{j=1}^{10^5} \cos \frac{t_j \ln n}{5}. \tag{9}$$

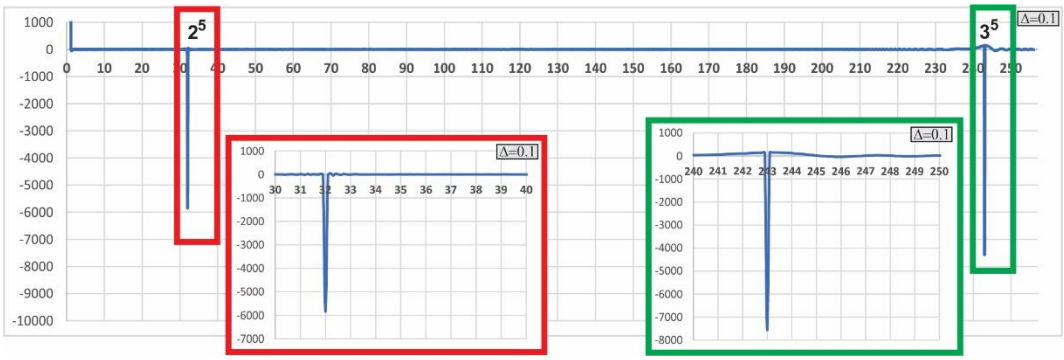

Figure 5. *RCS* of the fifth root.

The *RCS* of the sixth root of the argument n (10) is shown in Figure 6. The enlarged interval [60,70] highlights the resonance in 2^6:

$$RCS(\sqrt[6]{n}) = \sum_{j=1}^{10^5} \cos(t_j \ln \sqrt[6]{n}) = \sum_{j=1}^{10^5} \cos \frac{t_j \ln n}{6}. \tag{10}$$

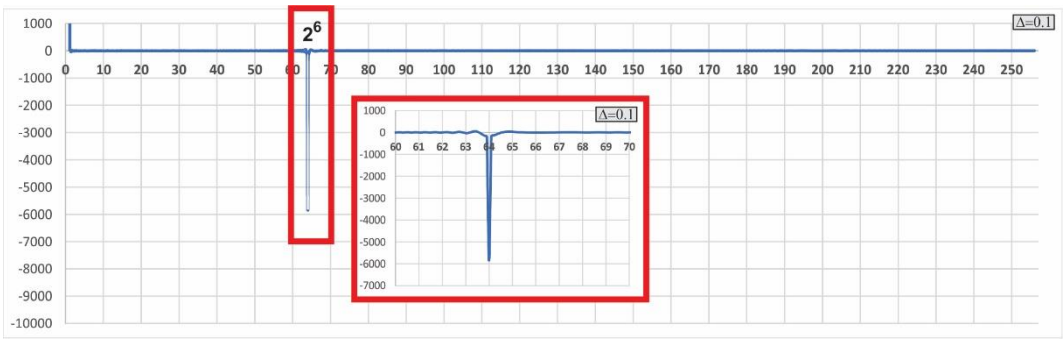

Figure 6. *RCS* of the sixth root.

The *RCS* of the seventh root of the argument of n (11) is shown in Figure 7. The enlarged interval [120,130] highlights the resonance in 2^7:

$$RCS(\sqrt[7]{n}) = \sum_{j=1}^{10^5} \cos(t_j \ln \sqrt[7]{n}) = \sum_{j=1}^{10^5} \cos \frac{t_j \ln n}{7}. \tag{11}$$

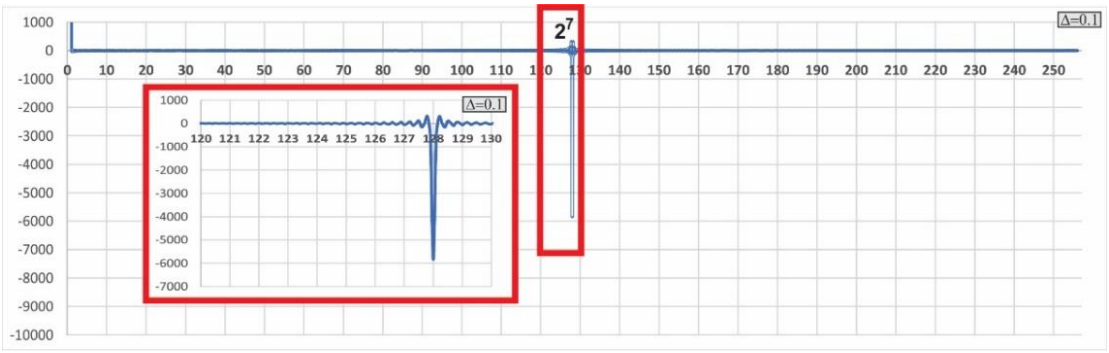

Figure 7. *RCS* of the seventh root.

Tables 2 and 3 display the calculated values of the *RCS* for primes from [2,256], from the first up to the eighth root. Number 1 is excluded from Table 2 as the counter function. RCS(1) is equal to the number of applied non-trivial zeros because $\ln 1=0 \Rightarrow \cos t_j \ln 1=1$. The columns of Table 2 contain the values of the root spectrum r for all prime numbers. Table 3 shows the values of the *RCS* for composite numbers.

Table 2. *RCS* of prime numbers in the interval [2,251].

	$RCS(\sqrt[k]{n})$							
n	r=1	r=2	r=3	r=4	r=5	r=6	r=7	r=8
2	**-5841.77**	-1.75	1.73	7.92	1.03	-3.19	-16.71	11.51
3	**-7562.81**	-0.37	-3.18	-0.53	-0.75	6.91	3.88	-0.45
5	**-8580.68**	-0.42	0.66	-3.66	4.80	-0.39	-3.43	-5.38
7	**-8768.19**	-0.90	3.70	-2.91	-2.81	4.63	-5.52	3.58
11	**-8619.67**	1.42	0.22	3.12	-0.32	1.62	-3.82	2.72
13	**-8481.29**	1.83	-0.09	3.03	-1.09	1.74	4.48	2.50
17	**-8191.98**	-0.82	2.73	4.03	-2.37	-1.09	4.07	-1.64
19	**-8055.32**	0.13	3.03	-0.34	-0.95	-1.79	-3.06	-3.94
23	**-7795.48**	-0.67	-2.05	1.19	-0.33	3.54	2.87	0.67
29	**-7455.07**	2.23	-0.04	1.02	6.05	-0.18	-0.02	-0.04
31	**-7351.99**	0.62	-0.05	-1.01	13.46	0.42	-1.32	2.73
37	**-7075.54**	1.16	1.38	2.74	-0.53	2.70	-0.11	2.57
41	**-6911.93**	1.64	1.62	2.80	2.38	2.81	-2.33	2.65
43	**-6834.79**	2.26	0.77	2.86	-0.65	-2.82	-0.19	2.46
47	**-6691.09**	-0.50	1.26	1.98	0.41	-0.12	0.82	-2.70
53	**-6498.83**	4.68	0.51	-0.07	0.84	4.89	2.92	-2.96
59	**-6325.45**	-0.77	-1.10	3.46	2.59	5.70	-2.37	-1.56
61	**-6272.48**	0.66	4.32	-1.35	-1.25	-6.83	-1.48	3.63
67	**-6120.73**	-1.92	0.22	4.00	1.05	0.51	2.11	2.78
71	**-6031.82**	2.40	0.51	4.81	-1.27	-2.85	3.57	-0.67
73	**-5984.87**	2.74	2.49	0.59	0.74	-1.54	0.28	-0.31

Continued to next page

$RCS(\sqrt[k]{n})$

n	r=1	r=2	r=3	r=4	r=5	r=6	r=7	r=8
79	**-5857.61**	0.39	2.69	4.41	2.11	-1.47	1.74	-2.55
83	**-5778.28**	-1.17	0.19	15.73	2.43	-0.40	3.76	3.43
89	**-5672.73**	0.14	0.79	3.74	-0.61	-0.41	2.25	3.15
97	**-5531.17**	0.51	1.99	**0.40**	-0.62	-0.72	-3.12	-1.91
101	**-5468.05**	-0.37	-0.99	**1.16**	2.80	-0.17	0.07	-1.89
103	**-5439.41**	-0.75	-0.51	0.52	0.94	-0.52	-1.64	2.23
107	**-5381.24**	-0.32	1.76	0.74	-0.73	-0.52	-3.98	-1.70
109	**-5349.80**	4.71	-1.34	0.38	1.28	1.69	4.76	0.88
113	**-5292.99**	5.51	-1.67	1.35	0.60	0.97	-5.49	3.53
127	**-5117.21**	2.87	-9.57	0.85	0.29	2.12	-55.26	3.69
131	**-5072.15**	1.28	-4.85	0.72	0.94	-1.25	-6.35	0.46
137	**-5003.31**	1.83	-1.86	1.04	3.02	-1.25	7.28	3.82
139	**-4981.15**	1.56	2.55	0.26	-1.11	-0.07	-3.22	-2.11
149	**-4881.91**	1.89	1.01	0.13	0.31	-0.69	3.19	2.56
151	**-4861.62**	1.54	1.09	0.79	2.96	2.04	-1.42	3.90
157	**-4805.68**	-0.39	1.97	0.15	3.35	-0.03	2.91	3.38
163	**-4753.54**	2.92	1.62	1.03	-1.73	1.77	1.62	4.07
167	**-4717.45**	4.02	0.35	0.02	0.55	2.63	2.18	3.04
173	**-4663.86**	0.36	1.34	0.74	-1.90	1.64	0.96	0.22
179	**-4615.21**	5.78	1.05	0.37	0.83	2.47	0.19	-3.05
181	**-4602.57**	1.69	0.62	-0.03	0.79	2.67	1.11	3.51
191	**-4533.44**	3.20	1.49	1.04	-2.66	2.14	1.18	0.38
193	**-4515.99**	3.44	0.71	1.37	-1.12	-1.03	-1.20	1.38
197	**-4480.22**	1.40	1.63	2.04	0.50	-0.43	-1.23	-2.05
199	**-4471.95**	0.70	1.32	2.00	-1.52	-1.05	-0.15	-3.11
211	**-4384.52**	1.51	1.54	-0.16	5.73	1.17	-0.96	-1.82
223	**-4311.33**	1.69	1.09	-0.67	6.92	0.25	-0.67	5.54
227	**-4285.30**	1.85	1.00	-0.81	-2.38	2.67	2.23	-5.05
229	**-4266.49**	1.98	1.36	-0.77	2.04	-1.28	1.76	-2.95
233	**-4256.51**	1.76	1.65	1.78	-12.29	2.30	-0.42	-7.55
239	**-4225.14**	2.49	1.66	4.06	16.95	-1.05	-0.43	-6.26
241	**-4205.19**	1.98	1.50	2.14	61.28	2.76	1.74	2.74
251	**-4148.67**	3.65	1.10	11.74	-13.45	1.07	2.20	-20.48

Table 3. *RCS* of prime powers in the interval [2, 251].

	$RCS(\sqrt[k]{n})$							
n	r=1	r=2	r=3	r=4	r=5	r=6	r=7	r=8
4	**-4130.47**	**-5841.77**	2.26	-1.75	1.93	1.70	1.07	7.92
8	**-2922.61**	-2.29	**-5841.75**	-2.25	2.21	-1.71	5.01	2.47
9	**-4363.91**	**-7562.81**	1.18	-0.37	-0.29	-3.15	-4.07	-0.53
16	**-2064.11**	**-4130.46**	2.79	**-5841.77**	2.36	2.23	-1.28	-1.75
25	**-3835.04**	**-8580.68**	3.67	-0.42	3.06	0.62	3.33	-3.66
27	**-2519.94**	3.49	-7562.74	0.82	-1.88	-0.43	3.88	0.90
32	**-1457.01**	1.58	0.47	1.01	**-5841.77**	-1.34	-2.51	-3.28
49	**-3309.02**	**-8768.19**	0.02	-0.90	2.14	3.73	1.10	-2.91
64	**-1029.77**	**-2922.61**	**-4130.39**	-2.29	2.60	**-5841.37**	2.62	-2.25
81	**-1451.83**	**-4363.91**	-0.28	**-7562.81**	0.67	1.21	-2.14	-0.37
121	**-2592.49**	**-8619.67**	-10.02	1.42	2.21	0.18	11.72	3.12
125	**-1716.03**	4.69	**-8580.48**	1.42	-1.23	-0.39	-15.39	-1.76
128	-727.76	-0.82	-12.83	0.50	2.99	-1.23	**-5841.77**	-0.01
169	**-2345.46**	**-8481.29**	1.50	1.83	-0.78	-0.12	-0.90	3.03
243	-833.63	2.91	1.70	-2.80	**-7562.82**	-0.96	2.35	11.78
256	-508.53	**-2064.11**	1.74	**-4130.46**	-7.23	2.78	0.02	**-5841.77**

From Tables 2 and 3, it is obvious that the inequality of the absolute resonance values of the *RCS* is satisfied (12) for all 15 prime powers from [2,256]. The calculations are given in Table 4.

$$\left|RCS(n)\right| < \left|\sum_{r=2}^{8} RCS(\sqrt[r]{n})\right|. \tag{12}$$

Table 4. Resulting *RCS* from (12).

n	$\left\|RCS(n)\right\|$		$RCS\sqrt[2]{n} + RCS\sqrt[3]{n} + RCS\sqrt[4]{n} + RCS\sqrt[5]{n} + RCS\sqrt[6]{n} + RCS\sqrt[7]{n} + RCS\sqrt[8]{n}$	$\left\|\sum_{r=2}^{8} RCS(\sqrt[r]{n})\right\|$
4	4130.47	<	5841.77 + 2.26 + 1.75 + 1.93 + 1.70 + 1.07 + 7.92	=5858.40
8	2922.61	<	2.29 + 5841.75 + 2.25 + 2.21 + 1.71 + 5.01 + 2.47	=5857.69
9	4363.91	<	7562.81 + 1.18 + 0.37 + 0.29 + 3.15 + 4.07 + 0.53	=7572.40
16	2064.11	<	4130.46 + 2.79 + 5841.77 + 2.36 + 2.23 + 1.28 + 1.75	=9982.64
25	3835.04	<	8580.68 + 3.67 + 0.42 + 3.06 + 0.62 + 3.33 + 3.66	=8595.44
27	2519.94	<	3.49 + 7562.74 + 0.82 + 1.88 + 0.43 + 3.88 + 0.90	=7574.14
32	1457.01	<	1.58 + 0.47 + 1.01 + 5841.77 + 1.34 + 2.51 + 3.28	=5851.96
49	3309.02	<	8768.19 + 0.02 + 0.90 + 2.14 + 3.73 + 1.10 + 2.91	=8778.99
64	1029.77	<	2922.61 + 4130.39 + 2.29 + 2.60 + 5841.37 + 2.62 + 2.25	=12904.13
81	1451.83	<	4363.91 + 0.28 + 7562.81 + 0.67 + 1.21 + 2.14 + 0.37	=11931.39
121	2592.49	<	8619.67 + 10.02 + 1.42 + 2.21 + 0.18 + 11.72 + 3.12	=8648.34

Continued to next page

n	$\lvert RCS(n)\rvert$		$RCS\sqrt[3]{n}+RCS\sqrt[4]{n}+RCS\sqrt[5]{n}+RCS\sqrt[6]{n}+RCS\sqrt[7]{n}+RCS\sqrt[8]{n}$	$\left\lvert\sum_{r=2}^{8} RCS(\sqrt[r]{n})\right\rvert$
125	1716.03	<	4.69 + 8580.48 + 1.42 + 1.23 + 0.39 + 15.39 + 1.76	=8605.36
128	727.76	<	0.82 + 12.83 + 0.50 + 2.99 + 1.23 + 5841.77+ 0.01	=5860.15
169	2345.46	<	8481.29 + 1.50 + 1.83 + 0.78 + 0.12 + 0.90 + 3.03	=8489.45
243	833.63	<	2.91 + 1.70 + 2.80 + 7562.82 + 0.96 + 2.35 + 11.78	=7585.32
256	508.53	<	2064.11 + 1.74 + 4130.46 + 7.23 + 2.78 + 0.02 + 5841.77	=12048.11

Based on the resonant values of the root *RCS* from Tables 2 and 3, and inequality (12), the resulting root *RCS* is formed (13). The graphic representation of the *RCS* results is given in Figure 8. Based on (13), the resonances of prime numbers p^1 in the interval [2,256] are located in the positive part and the resonances of all prime powers p^k, $k\in[2, 8]$ in the interval [2,256] are located in the negative part.

$$RCS(\sqrt[k]{n})=\sum_{j=1}^{10^5}\sum_{k=2}^{8}\cos(t_j\ln\sqrt[k]{n})-\sum_{j=1}^{10^5}\cos(t_j\ln n). \tag{13}$$

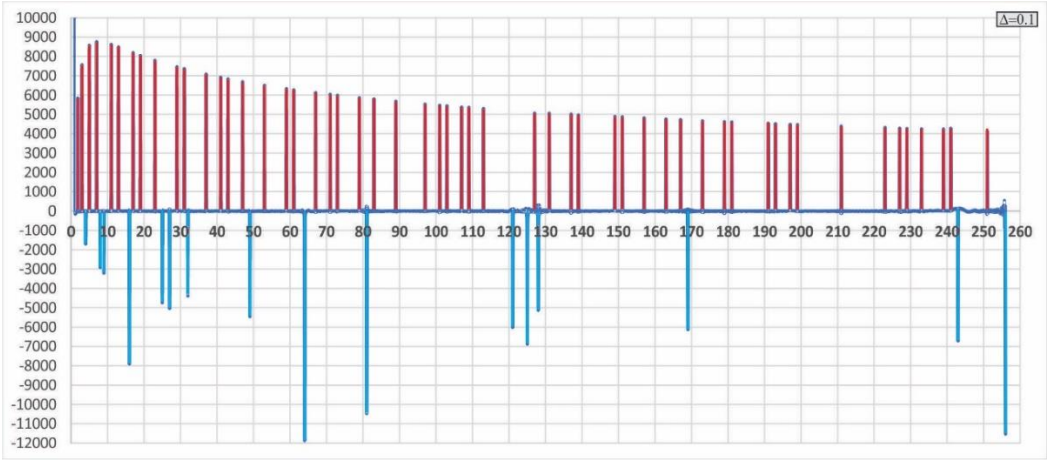

Figure 8. The resulting root RCS_R in the interval [2,256].

A subset of 54 numbers can be chosen from a set of 255 numbers in $1{,}840553\cdot10^{58}$ ways. Therefore, the reliability of choosing all prime numbers in the interval [2,256] in a random way is equal to $P=1-5.433148\cdot10^{-59}$. Based on this fact, we can claim that for all $n\in\mathbb{N}$, the following stands (14):

$$RCS_R(n)=\sum_{j=1}^{\infty}\sum_{k=2}^{\infty}\cos(t_j\ln\sqrt[k]{n})-\sum_{j=1}^{\infty}\cos(t_j\ln n). \tag{14}$$

Expression (14) can be transformed into the following (15):

$$RCS_R(n)=\sum_{j=1}^{\infty}\sum_{k=1}^{\infty}\cos(\frac{1}{k}t_j\ln n)-\sum_{j=1}^{\infty}2\cos(t_j\ln n). \tag{15}$$

The positive part of $RCS_R(n)$ contains the distribution of prime numbers.

3.3. Power RCS and magnitude of primes

The *RCS* of the second degree (16) is shown in Figure 9.

$$RCS(n^2)=\sum_{j=1}^{10^5}\cos(t_j \ln n^2)=\sum_{j=1}^{10^5}\cos(2t_j \ln n). \tag{16}$$

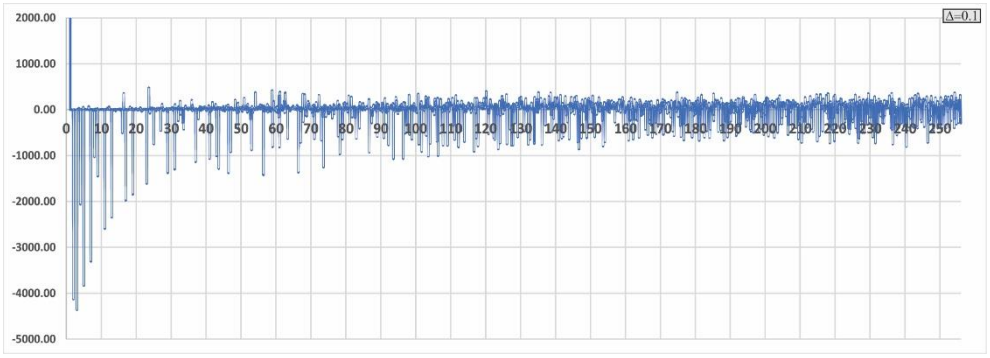

Figure 9. *RCS* of the second degree.

The apparent degradation of *RCS* resonances is a consequence of the small value of the increment Δ=0.1. Let us consider [2,4], [2,4]⊂*RCS*. It is obvious that resonant values are reached for 2, 3, and 4. Since the spectra that correspond to the powers compress the graph, the chosen value of Δ ought to be lowered. In that way, we obtain a more precise visualization of the segments of the concrete spectrum. On the other hand, changing values of Δ for the spectra that correspond to the roots is not needed.

Choosing Δ=0.00001 and enlarging the details, the observed resonance values correspond to the square roots of numbers 5, 7, 8, 11, and 13. Resonances in 2, 3, and 4 from *RCS* are the square roots of the composites 2^2=4, 3^2=9, and 4^2=16, respectively (Figure 10).

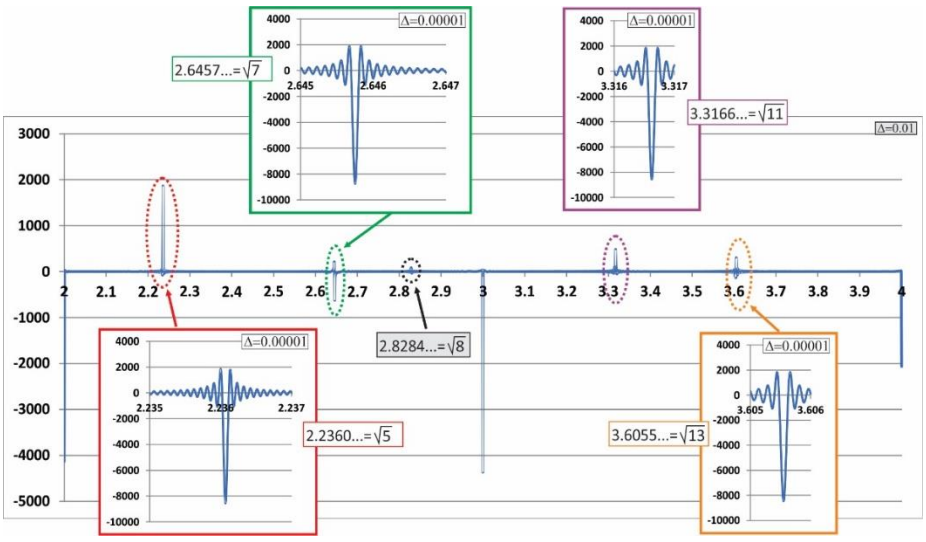

Figure 10. *RCS* of the second degree in [2,4] with enlarged details.

For example, in interval [200,202]⊂*RCS*, there are square roots of prime numbers from the interval [200^2,202^2] (i.e., [40000,40804]), with a total of 68 prime numbers: 40,009, 40,013, 40,031, 40,037, 40,039, 40,063, 40,087, 40,093, 40,099, 40,111, 40,123, 40,127, 40,129, 40,151, 40,153, 40,163, 40,169, 40,177, 40,189, 40,193, 40,213, 40,231, 40,237, 40,241, 40,253, 40,277, 40,283, 40,289, 40,343, 40,351, 40,357, 40,361, 40,387, 40,423, 40,427, 40,429, 40,433, 40,459, 40,471, 40,483, 40,487, 40,493, 40,499, 40,507, 40,519, 40,529, 40,531, 40,543, 40,559, 40,577, 40,583, 40,591, 40,597, 40,609, 40,627, 40,637, 40,639, 40,693, 40,697, 40,699, 40,709, 40,739, 40,751, 40,759, 40,763, 40,771, 40,787, and 40801. Figure 11 shows the interval [200,202] with an increment Δ=0.01. The total number of resonances in Figure 11 is 61 (i.e., 7 resonances of prime numbers from the interval [200,202] were not indicated by *RCS*).

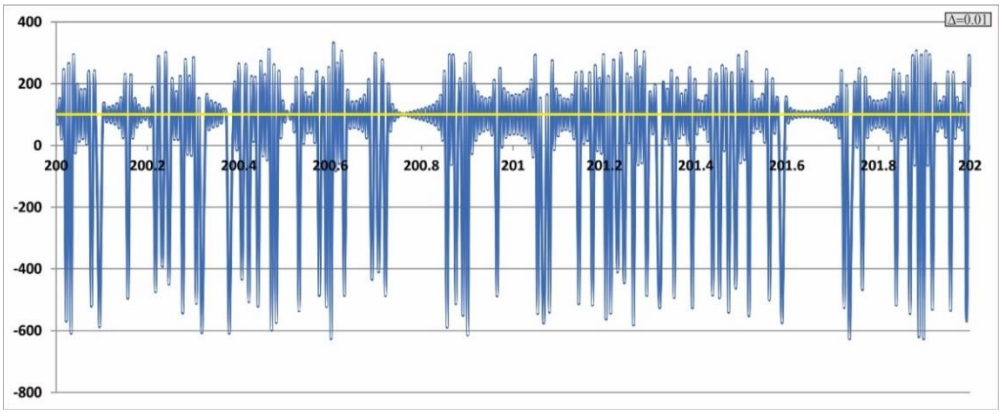

Figure 11. *RCS* of the second degree in [200, 202] with an increment Δ=0.01.

The *RCS* of the second degree obviously leads to a compression of the *RCS*. In order to emphasize the dynamics of the *RCS* development, we switch to the increment Δ=0.0001 and choose the interval [96,97]⊂*RCS*, which contains the square roots of prime numbers from the interval [96^2,97^2] (i.e., [9216,9409]), with a total of 21 prime numbers: 9221, 9227, 9239, 9241, 9257, 9277, 9281, 9283, 9293, 9311, 9319, 9323, 9337, 9341, 9343, 9349, 9371, 9377, 9391, 9397, and 9403. The number 97 is a prime, so we expect its appearance in the *RCS* as the square root of the composite 9409. All 21+1=22 resonances are visible in Figure 12.

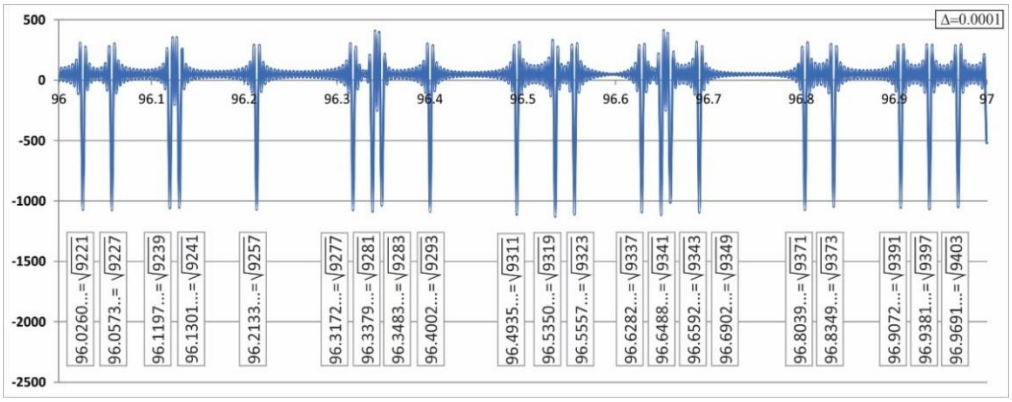

Figure 12. *RCS* of the second degree in [96,97] with an increment Δ=0.0001.

The enlarged details of the *RCS* are given in Figure 13. In the interval [96.60,96.70], there are square roots of four prime numbers 9337, 9341, 9343 and 9349 with the same increment; with the increment Δ=0.00001 in the interval [96.645,96.665], there are square roots of two prime numbers: 9341 and 9343.

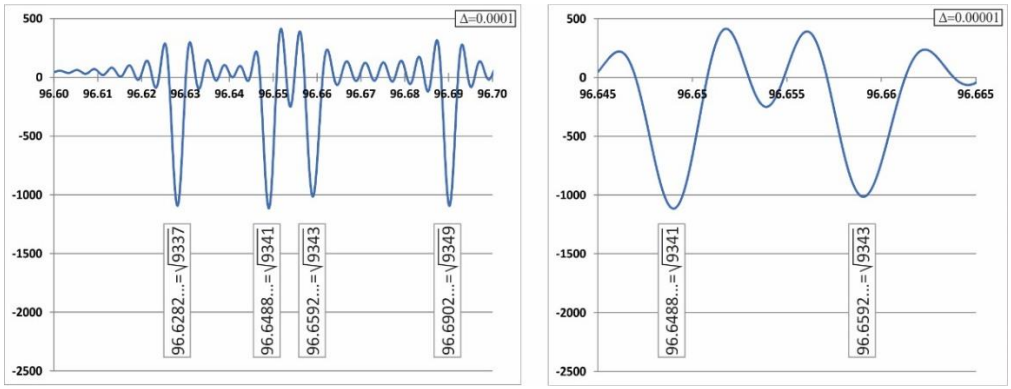

Figure 13. Enlarged details of the spectrum from Figure 12.

The *RCS* of the third degree (17) is shown in Figure 14.

$$RCS(n^3) = \cos\sum_{j=1}^{10^5} \cos(t_j \ln n^3) = \sum_{j=1}^{10^5} \cos(3t_j \ln n). \tag{17}$$

The expected third degree compression is obtained. For the applied increment Δ=0.1, two intervals were considered: [140,150] and [220,230] (Figure 14).

In [140,150], the cube roots of the prime numbers 2,967,361 and 3,163,577 in the positive part of the *RCS* and 3,254,959 in the negative part of the *RCS* are estimated. In [220,230], the prime number 11,512,561 was singled out in the positive part of the *RCS*.

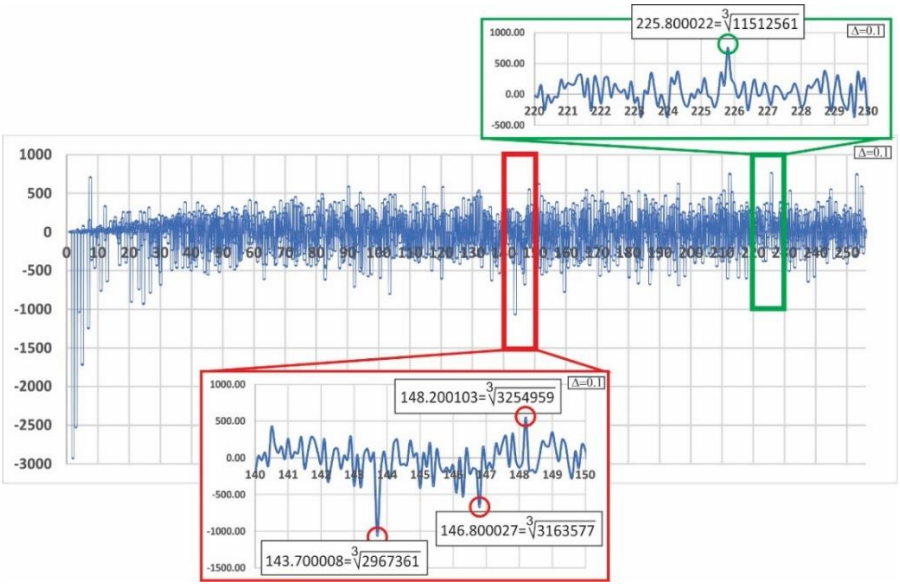

Figure 14. *RCS* of the third degree with enlarged details.

Applying the increment Δ=0.000005 on the left part of the Figure 15, parts of the *RCS* from [143.697,143.707] are selected, while three extreme values of the RCS that correspond to the cube root of the prime number 2,967,361 (from Figure 14) and two more cube roots of the prime numbers 2,967,379 and 2,967,397 are indicated.

However, in the interval [143.697^3, 143.7077^3] (i.e., [2,967,174.609, 2,967,794.117]), the cube roots of 48 prime numbers exist: 2,967,187, 2,967,199, 2,967,203, 2,967,221, 2,967,241, 2,967,247, 2,967,259, 2,967,269, 2,967,271, 2,967,277, 2,967,317, 2,967,323, 2,967,329, 2,967,331, 2,967,337, 2,967,343, 2,967,347, 2,967,353, 967,359, 2,967,361, 2,967,373, 2,967,379, 2,967,383, 2,967,389, 2,967,397, 2,967,403, 2,967,407, 2,967,409, 2,967,421, 2,967,427, 2,967,443, 2,967,491, 2,967,509, 2,967,551, 2,967,583, 2,967,607, 2,967,637, 2,967,647, 2,967,649, 2,967,689, 2,967,691, 2,967,697, 2,967,709, 2,967,737, 2,967,749, 2,967,751, 2,967,779, and 2,967,787.

Applying the increment Δ=0.000005 on the right part of the Figure 15, parts of the *RCS* from [225.796, 225.806] are selected, where only two resonant values that correspond to the cube root of the prime number 11,512,561 (selected from Figure 14) and only one more extreme value that may correspond to the cube roots of the prime numbers 11,513,263 or 11,513,269 are indicated.

Out of the established 90 prime numbers, only 6 are indicated in Figure 15. We can conclude that the intensity of the *RCS* of the third degree compression is high.

However, in the interval from [225.796^3,225.806^3] (i.e., [11511945.695,11513475.277]) there are 90 prime numbers: 11,511,947, 11,511,953, 11,511,961, 11,511,977, 11,511,979, 11,511,989, 11,512,013, 11,512,031, 11,512,037, 11,512,051, 11,512,073, 11,512,087, 11,512,093, 11,512,097, 11,512,147, 11,512,177, 11,512,199, 11,512,211, 11,512,219, 11,512,223, 11,512,231, 11,512,243, 11,512,301, 11,512,331, 11,512,337, 11,512,343, 11,512,363, 11,512,387, 11,512,399, 11,512,427, 11,512,481, 11,512,531, 11,512,541, 11,512,547, 11,512,561, 11,512,573, 11,512,601, 11,512,609, 11,512,649, 11,512,717, 11,512,733, 11,512,769, 11,512,789, 11,512,817, 11,512,843, 11,512,861, 11,512,901, 11,512,933, 11,512,937, 11,512,973, 11,512,981, 11,512,987, 11,512,999, 11,513,003, 11,513,009, 11,513,017, 11,513,039, 11,513,053, 11,513,057, 11,513,077, 11,513,141, 11,513,143, 11,513,149, 11,513,171, 11,513,189, 11,513,191, 11,513,209, 11,513,219, 11,513,239, 11,513,263, 11,513,269, 11,513,273, 11,513,279, 11,513,287, 11,513,291, 11,513,309, 11,513,311, 11,513,321, 11,513,329, 11,513,339, 11,513,371, 11,513,387, 11,513,393, 11,513,417, 11,513,419, 11,513,423, 11,513,429, 11,513,441, 11,513,461, and 11,513,473.

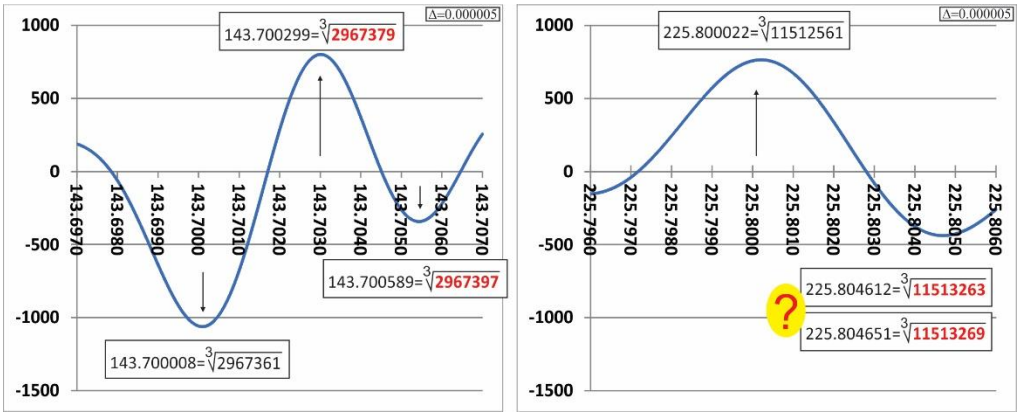

Figure 15. Enlarged detail from Figure 14.

Let us choose the *RCS* interval of the third degree from $1^3=1$ to $2^3=8$ since the lowest intensity of *RCS* compression in the initial part is expected. This interval contains the cube roots of the prime numbers 2, 3, 5, and 7 and the cube root of the composite number 4. On the selected interval, the increment $\Delta=0.1$ is chosen, while the increment $\Delta=0.0001$ is employed on the enlarged details of the *RCS*, shown in Figure 16.

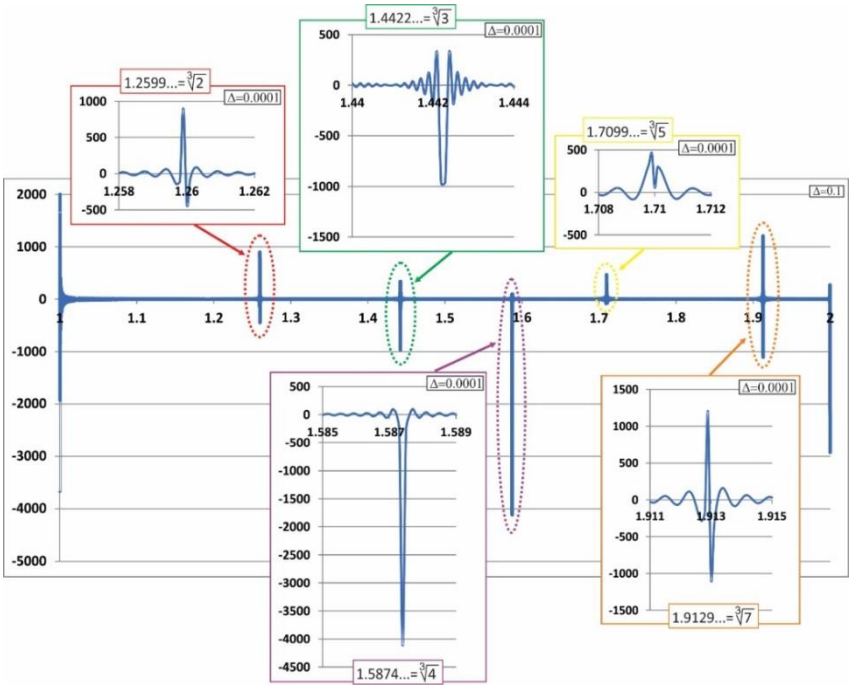

Figure 16. *RCS* of the third power interval [1,2].

Finally, we choose the *RCS* of the fourth degree (18) in the interval $[1^4,2^4]$ (i.e., [1,16]) since the lowest intensity of *RCS* compression in the initial part is expected. In this interval, there are the fourth roots of the prime numbers 2, 3, 5, 7, 11, and 13 and the fourth roots of the composite numbers 4, 8, and 9.

$$RCS(n^4)=\sum_{j=1}^{10^5}\cos(t_j \ln n^4)=\sum_{j=1}^{10^5}\cos(4t_j \ln n). \tag{18}$$

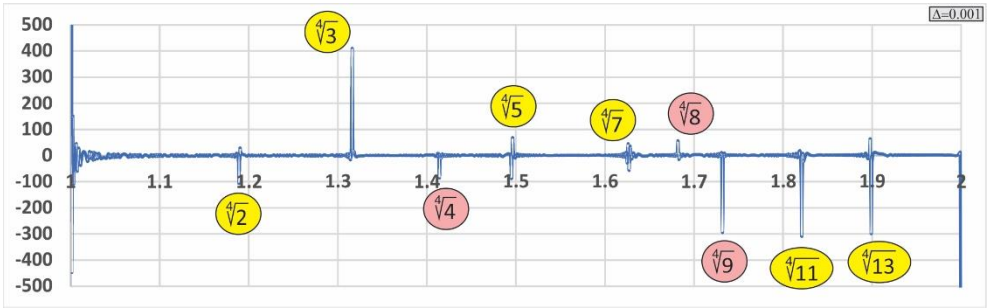

Figure 17. *RCS* of the fourth power interval [1,2].

Figure 18 shows the enlarged details of the *RCS* from Figure 17 with the increment Δ=0.00001.

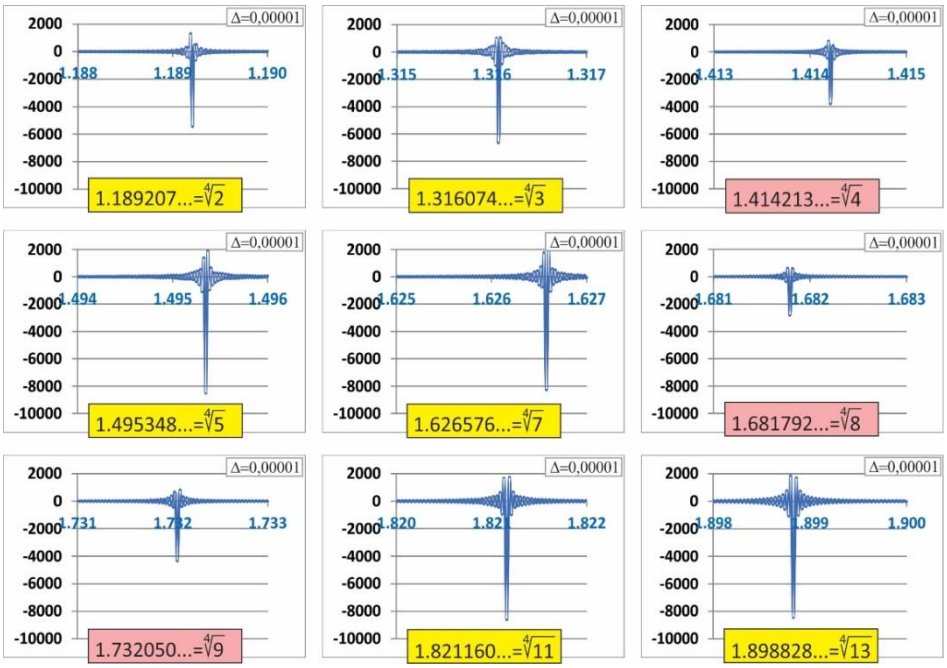

Figure 18. Enlarged details of the *RCS* from Figure 17.

It is obvious that the possibilities of further investigations are exhausted with the application of 10^5 complex parts of non-trivial zeros of the zeta function t_j. Higher power spectra are no longer available, regardless of the increment enhancement.

The power spectra can be used to calculate the magnitude of the p^d numbers from interval $[a^d,b^d]$. This magnitude is expressed in terms of the number of resonances on the interval $[a,b]$ of the spectrum of the d^{th} degree.

4. Imaginary sine spectrum-*ISS*

Let us consider the difference of the zeta functions from (3). We obtain the following (19):

$$\sum_{j=1}^{\infty}\frac{\zeta(0+it_j)-\zeta(0-it_j)}{2}=\frac{1}{2}\sum_{j=1}^{\infty}\sum_{n=1}^{\infty}\left(\frac{\cos(t_j\ln n)+i\sin(t_j\ln n)}{n^0}-\frac{\cos(t_j\ln n)-i\sin(t_j\ln n)}{n^0}\right)$$
$$=i\sum_{j=1}^{\infty}\sum_{n=1}^{\infty}\sin(t_j\ln n). \tag{19}$$

In Figure 19, the graph of the spectrum in the interval [1,256] is shown. The resonances of this spectrum change signs, where the value of the power of prime numbers p^k are most intense. Applying the increment Δ=0.1, the intensities of the resonances in *ISS* are 10 to 15 times lower than the resonances in the *RCS*. Some prime numbers do not have the expected resonances (example 239 from Figure 19). However, with a reduced increment to Δ=0.01, resonances appear in the *ISS* that are proportional to the resonances in the *RCS*. In general, *RCS* is far more stable than *ISS*. In the initial part, the intensity intensities of the resonances of numbers 2, 3, and 2^2 are extremely low.

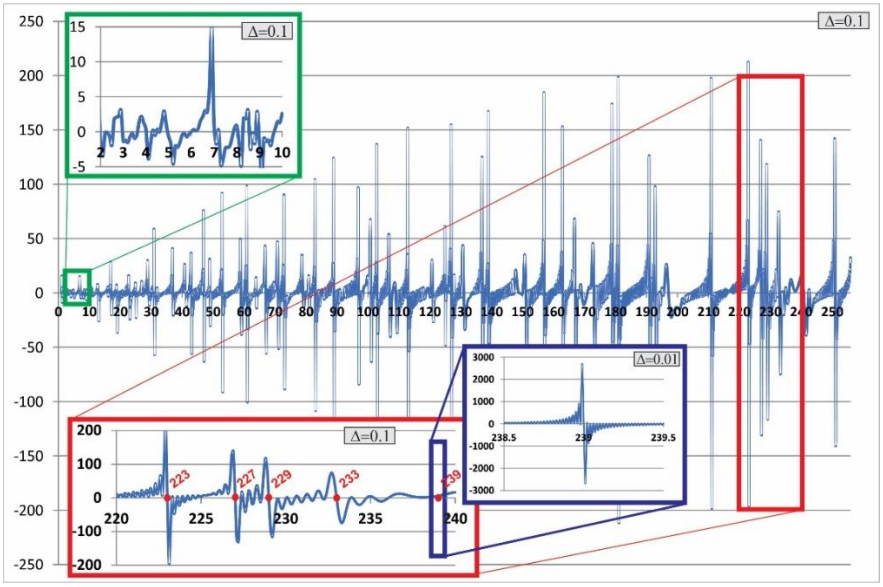

Figure 19. Imaginary sine spectrum with enlarged details.

From the number 5 onwards, the resonances in p^k are emphasized. The increment in Figure 20 is Δ=0.001.

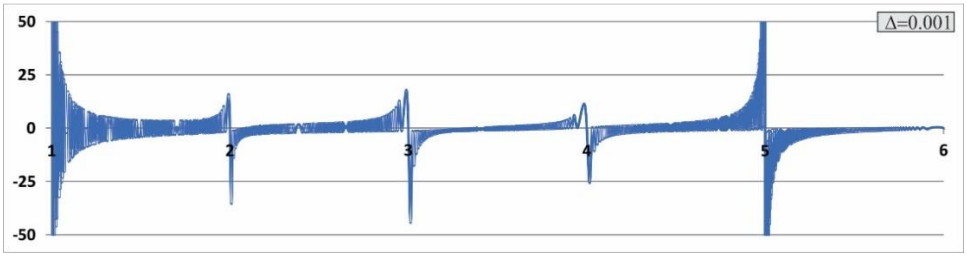

Figure 20. Low level resonances of numbers 2, 3 and 4 for the first 100000 non-trivial *ISS* zeros.

Moreover, the *ISS* has root and power spectra. Analogously to (16), a new resulting spectrum (20) can be formed as follows:

$$ISS_R(n) = \sum_{j=1}^{10^5} 2\sin(t_j \ln n) - \sum_{j=1}^{10^5}\sum_{k=1}^{3} \sin(\frac{t_j}{k} \ln n). \tag{20}$$

In Figure 21, the interval [22,30] is shown. In the interval, there are two prime numbers, specifically 23 and 29, the second power of the prime number $25=5^2$, and the third power of the prime number $27=3^3$. Representations of the basic *ISS* and its second and third roots for the increment Δ=0.005 are given. The resulting spectrum (24) contains orthogonal resonances. Figure 21 leads us to the conjecture that the values of the resultant *ISS* in the values of the root $r \in \mathrm{N}$ are asymptotes.

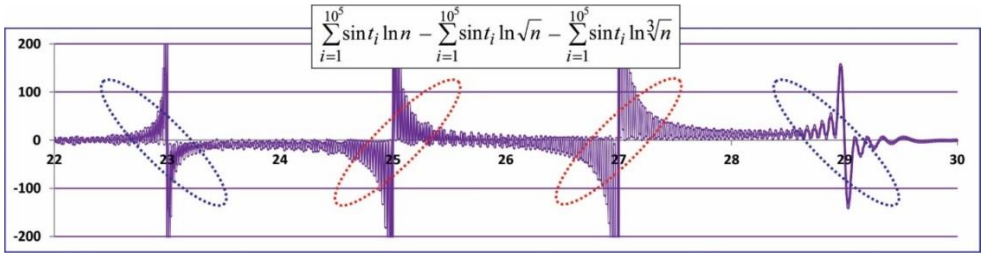

Figure 21. *ISS* of roots, interval [22,30].

There is a clear distinction between prime numbers and composites p^r (21).

$$ISS_R(p^r)=\sum_{j=1}^{\infty}\sin(t_j\ln n)-\sum_{j=1}^{\infty}\sum_{r=1}^{\infty}\sin(t_j\ln\sqrt[r]{n})=\pm\infty \qquad \begin{cases} r=1 & \lim\limits_{\varepsilon\to 0} ISS_R(p^r\mp\varepsilon)=\pm\infty, \\ r\geq 2 & \lim\limits_{\varepsilon\to 0} ISS_R(p^r\mp\varepsilon)=\mp\infty. \end{cases} \tag{21}$$

5. Composite spectrum

The sum of the resultant cosine (15) and sine (20) spectra superposes the resonances. In that manner, a composite spectrum of the distribution of all degrees of prime numbers is obtained as follows (22):

$$\pi(p^k)=\left|\sum_{j=1}^{\infty}\cos(t_j\ln n)\right|+\left|\sum_{j=1}^{\infty}\sin(t_j\ln n)\right|-\left|\sum_{j=1}^{\infty}\sum_{r=1}^{\infty}\cos(t_j\ln\sqrt[r]{n})\right|-\left|\sum_{j=1}^{\infty}\sum_{r=1}^{\infty}\sin(t_j\ln\sqrt[r]{n})\right|. \tag{22}$$

In Figure 22, the composite spectrum for the first 100,000 non-trivial zeros (22) from the interval [120,140] is shown. That interval contains four prime numbers: 127, 131, 137, and 139, as well as three degrees of prime numbers: $121=11^2$, $125=5^3$, and $128=2^7$. Figure 22 separates composite resonances for p^1 and p^r, $r\geq 2$ primarily by sign. Additionally, the shapes of the resonances for p^1 and p^r, $k\geq 2$ significantly.

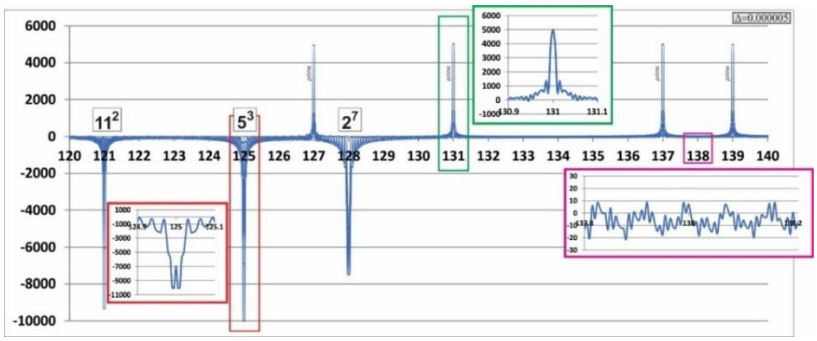

Figure 22. Composite spectrum on the interval [120,140] with enlarged details.

6. Conclusions

The previous considerations of the cosine spectrum based on the values of the complex part of

non-trivial zeros were significantly improved by the presented results. First, the genesis of the real cosine spectrum was established.

Second, a simple relationship between non-trivial zeros and the distribution of prime numbers based on the root spectrum was established.

Finally, a system to determine the magnitude of the p^k based on the degree spectrum was established.

The obtained spectra indicate that the values of the zeta function are also important outside the critical axis, specifically for $\sigma=0\neq½$. The discussion of possible non-trivial zeros outside the critical axis $\sigma=½$ is irrelevant to the results in the paper. The obtained spectra are based on the values of non-trivial zeros from the Riemann hypothesis, and the established distribution of prime numbers based on the spectra supports the famous hypothesis. In addition to the distribution of prime numbers, the spectra highlight magnitudes of prime numbers.

Further research should be directed towards increasing the numerical sharpness applying more non-trivial zeros and reducing the increment. Additionally, the spectra of the negative domain $RCS(-n)$ and $ISS(-n)$ should be investigated using hyperbolic sine and cosine functions.

Author contributions

Ilija Tanackov: Conceptualization, investigation, methodology, formal analysis, figure preparation, writing–original draft preparation; Ivan Pavkov: Conceptualization, writing–original draft preparation, validation, writing–original draft preparation; Dejan Ćebić: Methodology, numerical analysis, figure preparation, validation; Željko Stević: Visualisation, validation, writing–review and editing. All authors have read and agreed to the published version of the manuscript.

Use of Generative-AI tools declaration

The authors declare that they have not used Artificial Intelligence (AI) tools in the creation of this article.

Acknowledgments

This research has been supported by the Ministry of Science of the Republic of Serbia within the Project: Innovative scientific and artistic research in the domain of FTN activities, University of Novi Sad, Faculty of Technical Sciences.

Conflicts of interest

The authors declare no conflict of interest.

References

1. C. L. Siegel, Uber Riemanns Nachlaß zur analytischen Zahlentheorie, *Quellen Stud. Gesch. Math. Astron. Phys. Abt. B*, **2** (1932), 45–80.
2. J. P. Gram, Note sur les zeros de la fonction de Riemann, *Acta Math.*, **27** (1903), 289–304. https://doi.org/10.1007/BF02421310

3. J. I. Hutchinson, On the roots of the Riemann zeta function, *T. Am. Math. Soc.*, **27** (1925), 49–60. https://doi.org/10.2307/1989163
4. E. C. Titchmarsh. The zeros of the Riemann zeta-function. *Proc. A*, **157** (1936), 261–263. https://doi.org/10.1098/rspa.1936.0192
5. D. H. Lehmer, On the roots of the Riemann zeta-function, *Acta Math.*, **95** (1956), 291–298. https://doi.org/10.1007/BF02401102
6. R. S. Leghman, Separation of zeros of the Riemann zeta-function, *Math. Comput.*, **20** (1966), 523–541. https://doi.org/10.1090/S0025-5718-1966-0203909-5
7. J. B. Rosser, J. M. Yohe, L. Schoenfeld, *Rigorous computation and the zeros of the Riemann zeta-function*, In: Proceedings of IFIP Congress, **1** (1968), 70–76.
8. R. P. Brent, The first 40,000,000 zeros of ζ(s) lie on the critical line, *Notices Am. Math. Soc.*, **24** (1977), 417–477.
9. R. P. Brent, J. V. D. Lune, H. J. J. T. Riele, D. T. Winter, On the zeros of the Riemann zeta function in the critical strip, II, *Math. Comput.*, **39** (1982), 681–688. https://doi.org/10.1090/S0025-5718-1982-0669660-1
10. J. V. D. Lune, H. J. J. T. Riele, D. T. Winter, On the zeros of the Riemann zeta function in the critical strip, IV, *Math. Comput.*, **46** (1986), 667–681. https://doi.org/10.2307/2008005
11. S. Wedeniwski, *Zetagrid-computational verification of the Riemann hypothesis*, In: Conference in Number Theory in Honour of Professor H.C. Williams, Alberta, Canda, May 2003.
12. D. Platt, T. Trudgian, The Riemann hypothesis is true up to $3 \cdot 10^{12}$, *B. Lond. Math. Soc.*, **53** (2021), 792–797, https://doi.org/10.1112/blms.12460
13. E. C. Titchmarsh, *The Zeta-function of Riemann,* Cambridge University Press, 1930.
14. A. Kawalec, The recurrence formulas for primes and non-trivial zeros of the Riemann zeta function, *arxiv Preprint*, 2021. https://doi.org/10.48550/arXiv.2009.02640
15. B. Mazur, W. Stein, *Primes: What is Riemann's hypothesis?* Cambridge University Press, 2016.
16. E. Hasanalizade, Q. Shen, P. J. Wong, Counting zeros of the Riemann zeta function, *J. Number Theory*, **235** (2022), 219–241. https://doi.org/10.1016/j.jnt.2021.06.032
17. E. P. Balanzario, A note on the distribution of clusters and deserts of prime numbers, *Indagat. Math.*, **5** (2025), 1276–1287. https://doi.org/10.1016/j.indag.2025.03.007
18. M. C. Hugill, Primes between consecutive powers, *J. Number Theory*, **247** (2023), 100–117. https://doi.org/10.1016/j.jnt.2022.12.002
19. Y. Matiyasevich, Towards non-iterative calculation of the zeros of the Riemann zeta function, *Inf. Comput.*, **296** (2024), 105130. https://doi.org/10.1016/j.ic.2023.105130
20. V. Starichkova, A note on zero-density approaches for the difference between consecutive primes, *J. Number Theory*, **278** (2026), 245–266. https://doi.org/10.1016/j.jnt.2025.04.007
21. E. Madison, P. A. Madison, S. V. Kozyrev, Aperiodic crystals, Riemann zeta function, and primes, *Struct. Chem.*, **34** (2023), 777–790. https://doi.org/10.1007/s11224-022-01906-2

AIMS Press